Direct Absorption Volumetric Molten Salt Receiver With Integral Storage

Citation: Codd, Daniel S., and Alexander H. Slocum. "Direct Absorption Volumetric Molten Salt Receiver With Integral Storage." Proceedings of the ASME 2011 5th International Conference on Energy Sustainability, 7-10 August, 2011, Washington, DC, USA, ASME, 2011. © 2011 by ASME

As Published: http://dx.doi.org/10.1115/ES2011-54175

Publisher: ASME International

Persistent URL: http://hdl.handle.net/1721.1/120988

Version: Final published version: final published article, as it appeared in a journal, conference proceedings, or other formally published context

Proceedings of the ASME 2011 5th International Conference on Energy Sustainability
ES2011
August 7-10, 2011, Washington, DC, USA

ES2011-54175

DIRECT ABSORPTION VOLUMETRIC MOLTEN SALT RECEIVER WITH INTEGRAL STORAGE

Daniel S. Codd[1]
codd@mit.edu

Alexander H. Slocum
slocum@mit.edu

Department of Mechanical Engineering, Massachusetts Institute of Technology
Cambridge, MA, US

ABSTRACT

A new design is presented for a concentrating solar power central receiver system with integrated thermal storage. Concentrated sunlight penetrates and is absorbed within a passive molten salt pool, also acting as a single-tank assisted thermocline storage system. The receiver has a relatively small aperture, open to the environment without requiring a transparent window to isolate the system, exhibiting low losses while achieving high temperatures needed for efficient power generation. The use of an insulated divider plate provides a physical and thermal barrier to separate the hot and cold salt layers within the receiver. The position of the divider plate is controlled throughout the day to enhance the natural thermocline which forms within the salt. As a result, continuous, high temperature heat extraction is possible even as the average temperature of the salt is declining. Experimental results are presented for an optically heated 5 L capacity sodium-potassium nitrate salt volumetric receiver equipped with a movable divider plate.

NOMENCLATURE

I_o	incident intensity
I	transmitted intensity
α	attenuation coefficient
δ	optical thickness

INTRODUCTION

There are numerous Concentrated Solar Power (CSP) receiver designs in the realm of point focus solar power towers, each attempting to address the functional requirements of capturing and converting concentrated sunlight into usable, high temperature heat. Conventional surface absorption tube-based receivers have been studied and tested, only to exhibit moderate capture efficiencies, parasitic fluid pumping losses and raise long term durability concerns [1-3].

Direct Absorption Receivers (DARs) can reduce radiative and convective losses to the environment while increasing operating temperature and capture efficiency [4]. Volumetric absorption in a DAR reduces the susceptibility of receiver overheating and failure due to transient solar fluctuations. Several designs have been tested, including volumetric air receivers and cascading molten salt waterfalls. Absorption into molten salts with high volumetric heat capacities enables simple subsequent thermal storage. However, experiments using centimeter-thick molten salt waterfall films were found to be marginally absorbing to incoming sunlight, and needed to be doped with high absorptivity particles to collect the required energy within the salt film [5]. Unfortunately, the exposed active fluid flow and variations in temperature as a function of varying solar flux, and the cost of pumps, manifold and piping preheaters limits the practicality of such systems [6].

Alternative approaches, such as Rabl's beam down system, seek to relocate the receiver to ground level to avoid some of the tower-based receiver constraints [7]. For example, Epstein and Segal proposed an integrated receiver/storage tank whereby molten salt flows in a double-wall conical cavity located at ground-level [8]. Additionally, a ground-level receiver enables

[1] Corresponding author; codd@mit.edu, (617) 253-4917
Massachusetts Institute of Technology, 77 Massachusetts Avenue, Room 3-438, Cambridge, MA 02139-4301 USA

the use of novel materials and geometries for receiving concentrated sunlight–notably a liquid free surface [9,10]. However, beam down optics are costly, incur additional reflection losses and pose high-flux durability issues. Actively cooled tertiary concentrators are needed to compensate for the increased sun spot size due to the increased focal length created by the beam-down geometry. Also, the use of quartz aperture windows to isolate the receiver chamber reflects and absorbs a portion of the incident energy and raise long term durability concerns [11,12].

Regardless of the receiver design, CSP systems benefit from thermal storage for dispatchable energy production. Current systems utilize remote thermal storage of various designs: tanks of pumped molten nitrate salts, banks of oil-filled steel pipe bundles encased in concrete, or hot-air heated hollow refractory brick chambers [13]. These designs require an active heat-transfer fluid flow, with associated high-temperature pumping issues and costs. Long molten salt piping runs require heat tracing and control systems to prevent freezing; however, despite these measures major operating problems still occur [14-16]. For example, the Solar Two CSP demonstration plant was disabled by frozen salt in pipes even with ancillary heaters, required for daily preheating and filling of the receiver [2].

For widespread adoption, CSP designs must show improved efficiency, robustness, energy storage and exhibit low capital and operating costs. Designs capable of increased working fluid temperatures will be favored for the resulting flexibility in choosing and improvements in power cycle efficiencies.

CSPOND CONCEPT

Here we present a high-temperature CSP system with integral energy storage, whereby concentrated light is beamed through an aperture directly into a large molten salt filled thermal receiver. The light that enters this salt pond will penetrate, scatter, and be absorbed through the volume of salt, rather than on a surface. The salt pond will act as a buffer between the diurnal and instantaneous variations of the heliostat field's solar flux and the power generation unit – providing dispatchable Concentrated Solar Power on Demand (CSPonD) [17,18].

Figure 1 depicts a schematic of the CSPonD system. Heliostats mounted on a hillside beam light directly into a molten salt receiver at the base of the hill. This eliminates costly beam-down optics, reflective losses and a tall receiver tower. Cosine effect losses associated with hillside heliostats beaming light downwards to the receiver are offset by the elimination of a tower and separate hot and cold storage tanks and their associated pumping systems. Noone et al. describes a hillside site selection tool applied to a case study of the entire western United States, finding numerous sites with natural sloped terrain and high solar insolation, ideal for development with the CSPonD system [19]. Methods developed by utility companies for emplacing utility poles on moderately steep terrain can be used for heliostat installation, and automated spray systems can be utilized for cleaning the mirrors.

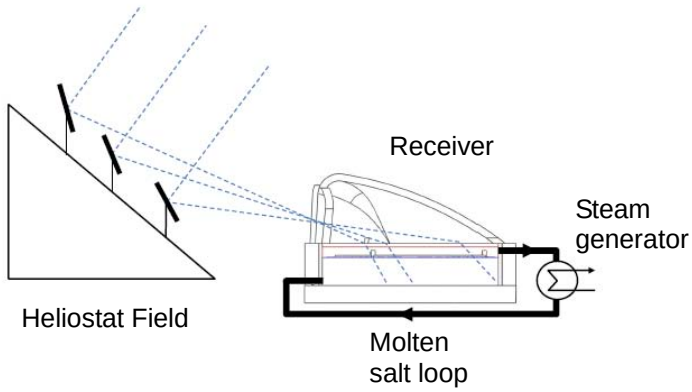

Fig. 1: CSPonD beam-down system architecture

Volumetric Absorption Receiver

Concentrated solar flux passing through the aperture can follow one of three paths: refracted into the molten salt; reflected off the salt surface towards the inside surface of the receiver lid; or directly impinged on the inner surface of the lid (Fig. 2). The energy that is transmitted through the salt will decay as a function of the optical path length, δ, according to the Beer-Lambert law:

$$I = I_0 e^{-\alpha\delta} \tag{1}$$

Experimentally obtained values for the attenuation coefficient, α (cm^{-1}), which includes both absorption and scattering, for molten salts of interest are on the order of 0.01 cm^{-1} over the visible spectrum [20]. For example, a 5 m path length through molten salt would absorb 99% of the incoming concentrated visible radiation.

The hillside heliostat field allows for direct entry into the molten salt pond for a majority of rays; any that are reflected or off-target can be redirected or absorbed by a grazing incidence, non-imaging cover over the pond. This cover serves two additional purposes: to reduce radiative losses to the environment and to condense a majority of the vaporized salt which otherwise would be carried away. If cooled, a layer of highly reflective and insulating solidified salt can form on the inside of the refractory-lined cover which serves to further insulate the pond and reflect visible radiation into the molten salt. Thus the CSPonD receiver can provide two heat extraction loops: low temperature from actively cooling the pond cover, and high temperature directly from the heated molten salt. These can be optimally controlled to maximize power output, even when the sun is not shining. The low temperature pond cover heat may be used for both power cycle and brine preheat in collocated power/desalination plants [21].

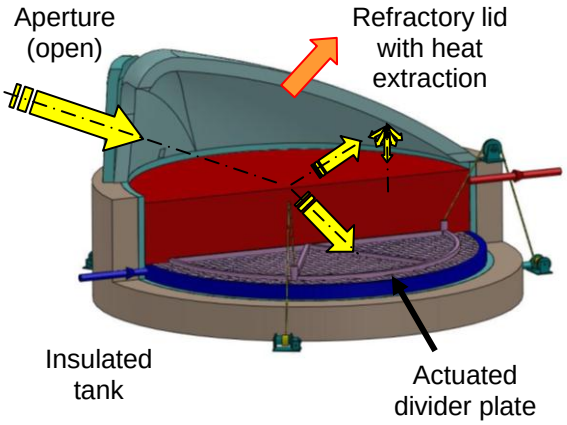

Fig. 2: CSPonD receiver cutaway view

Lid and salt pond temperatures are just some of the key parameters needed to characterize a CSPonD receiver. Others include input flux concentration, nominal pond diameter and average beam down angle of the incoming concentrated light. Aperture size is driven by system sizing and input flux concentration, and is used to calculate the system's geometrical view factors needed for accurate radiative loss estimates to the environment. A first-order collection efficiency analysis is presented in *Annex A*. Capture efficiency increases with input flux concentration; the self-healing nature of the molten salt surface tolerates higher fluxes than conventional tube based receivers–and can achieve greater efficiencies as heliostat field technology and achievable concentration improves. However, these efficiency calculations have assumed that there is no mass transfer across the aperture; a real system is expected to have additional losses from the lid to the environment. Nevertheless, the unique dual heat-source nature of the salt and lid in CSPonD receivers will allow more flexibility for operators to maximize useful heat extraction for their particular system.

Materials Durability & Construction

There is a wealth of knowledge in regards to salt bath furnace construction and operation, whereby large vats of molten salts open to the atmosphere are used in the thermal processing of metals [22]. Low-cost eutectic salt mixtures achieve the desired operating ranges: low temperature (130-600°C) quenching/tempering nitrate-nitrite and nitrate salts; high temperature (400-800°C) tempering/drawing carbonate salts; and neutral high-speed hardening (850-1100°C) chloride salts. Typical high temperature salt baths utilize internal mortarless refractory firebrick insulation, followed by a carbon steel shell and external ceramic fiber insulation. A "freeze plane" is formed within the alumina-silica firebrick, and as a result, carbon steel tank walls are not exposed to the corrosive molten salt. The tank lid and aperture structure can be located so high intensity refracted light does not impinge directly on the tank wall refractory liner and cause undue thermal strains.

The heat treating industry has developed standard methods to test and control the salt chemistry using chemical rectifiers and periodic removal of metallic oxides which settle to the bottom of the tank. The rate of impurity buildup will be much lower for CSPonD than for a heat treating bath with its daily throughput of steel parts. Regardless, it is anticipated that impurities in suspension will have a significant effect on the attenuation properties of the salt and will therefore have to be closely monitored and controlled.

A promising salt candidate for the CSPonD receiver is sodium-potassium nitrate (i.e., solar salt: 60/40 wt.% $NaNO_3$-KNO_3) which has a low melting point of 222°C. Above 593°C solar salt decomposes and becomes corrosive and dangerous; however commercial systems have been built to pump it between hot and cold storage tanks and a steam generator [23]. The power block, including salt pumps, heat exchanger/steam generator & power generation unit for a nitrate salt based CSPonD system are similar to those that can be commercially obtained. Hence, for a nitrate salt CSPonD system, a steam power cycle can be assumed with peak steam temperatures of 500-540°C.

Low-cost chloride salt mixtures can be utilized in a high temperature, high efficiency CSPonD system. For example, a NaCl-KCl (50/50 wt.%; melting point 660°C) CSPonD, operating from 700-1000°C, could easily power a supercritical CO_2 power cycle. The power extraction system in high temperature designs can be leveraged from salt handling and power cycle technology required for the molten salt reactor (MSR), part of the Aircraft Nuclear Propulsion Program [24].

The lid and closeable aperture doors can be lined with lightweight insulating refractory board; both the molten salt pond and the lid will exchange heat with each other and to the environment by convection, radiation and conduction. As mentioned previously, the cover can be backside cooled to enhance the buildup of salt that condenses on the inner surface of the cover, akin to frost collecting on evaporator coils within a refrigerator. The solidified salt/lid interface is expected to act as a diffuse reflector to incoming light that reflects off the surface of the salt. However, the salt vapors would also condense on the inner surface of quartz aperture window, reducing its effective transmission. This fogging is a primary reason why a quartz window for the aperture is not being considered; if needed, air-curtains can be employed to limit mass and heat transfer while the aperture is open.

Integral Divided Thermocline Storage

A corrosion and creep resistant alloy "divider plate" axially separates the top (hot) and bottom (cold) salt sections of the tank (Fig. 2). The divider plate is well insulated and near-neutrally buoyant, providing a physical and thermal barrier between the thermally stratified hot and cold layers within the tank. Its position is controlled axially to maintain the hot and cold salt volumes required for continuous operation. Hot salt is extracted from the top of the receiver tank, sent to a steam

generator and returned to the bottom of the receiver tank at a lower temperature.

There is a generous annular clearance between the divider plate edge and tank walls. This clearance prevents binding and allows for annular salt flow past the plate during daytime charging of the system, where colder salt from below moves past the annular clearance space between the barrier plate and tank wall to be reheated. Incoming light penetrates deeply and a portion of it will be absorbed on the divider plate causing convection currents, heating the hot salt to a uniform high temperature. As the system collects more energy and the top hot section grows in thickness, the divider plate is lowered in the tank. Nighttime energy extraction is accomplished by raising the divider plate, following the natural thermocline progression upward as the hot salt volume decreases. As a result, high-temperature steam can be provided even as the average temperature of the salt in the tank decreases.

Copeland et al. [25,26] has shown "passive rafted thermocline" designs effective at boosting thermal stratification in water tanks, with suggested designs for molten salt thermal storage tanks. However, passive rafted thermoclines would rely on two parameters difficult to control in high temperature molten salt tanks: maintaining neutral buoyancy at the hot-cold thermocline interface; and a near perfect seal with the side walls to prevent leakage around the divider raft. An additional element of operational control is gained by actuating a near-neutrally buoyant divider plate, avoiding raft instabilities and jamming failures. Thin gauge corrosion-resistant liners can be used to reduce thermal shock to the internal firebrick from fluctuating salt levels, as demonstrated in CSP hot salt storage tank designs [16].

The amount of storage required depends on local needs and economic conditions. Assuming a 300 K temperature swing, solar salt provides roughly 540 kJ/kg or 240 kW_th/m^3 sensible heat storage. With a conservative thermal-to-electric conversion efficiency of 30%, one can assume it takes about 14 $m^3/MW_e/h$ of nitrate salt for non-sunshine operation. For example, 2500 m^3 of salt can provide 180 MW_eh of energy storage, capable of powering a 50 MW_e turbine for 3.6 hours without additional solar input. This volume of salt can be contained in a 5 m deep, 25 m diameter CSPonD receiver. Obviously, supplying a large power cycle will require a large heliostat field, necessitating a large receiver aperture with increased losses. However, local economic conditions may dictate mid-afternoon and early evening power production – whereby a smaller heliostat field can charge a CSPonD receiver throughout the morning and then used to meet demand. The CSPonD system is rated by continuous power production, not peak power as is typical of traditional CSP systems without thermal storage.

EXPERIMENTAL TESTING

A high-flux large-area solar simulator was designed to achieve output fluxes greater than 60 kW/m^2 to test lab-scale CSPonD receivers [27]. While 60-sun simulator testing is not sufficient for quantitative high temperature receiver operation or controlled heat extraction measurements, it provides qualitative insights into volumetric absorption behavior and convective mixing effects.

Single Tank System

Optical heating tests of a single tank, volumetric molten salt receiver were performed to determine the temperature distribution of commercial grade Hitec® solar salt: 60/40 wt.% $NaNO_3$-KNO_3. A well-insulated stainless steel (type 316L) receiver, 67mm inner diameter x 250 mm high was used to contain the salt. The salt was premelted to 250°C, and then optically heated with MIT CSP solar simulator. Thermal stratification was observed, although the upper third of the salt was nearly at the same temperature as the surface, indicating volumetric energy absorption and convective mixing throughout that region of the receiver.

Divider Plate Tank System

Additional tests were carried out using a receiver equipped with a movable divider plate, designed to partition the volumetric molten salt receiver into two thermally separated regions. The type 316L stainless steel receiver was designed with proportions similar to the aforementioned 50 MW_e receiver: 280 mm inner diameter x 80 mm high, and the interior was instrumented at several locations with type K thermocouples (Fig. 3). The divider plate was constructed with an 8 mm annular clearance to the tank walls from 3.2 mm thick 316L stainless steel with a 6.4 mm thick layer of rigid silica insulation board affixed to the underside. 5 L of commercial solar salt was premelted to 250°C and optically heated with MIT CSP solar simulator. The tank was well-insulated radially and placed on top of a 101.4 mm slab of calcium silicate insulation, which rested on a catch basin on the concrete lab floor.

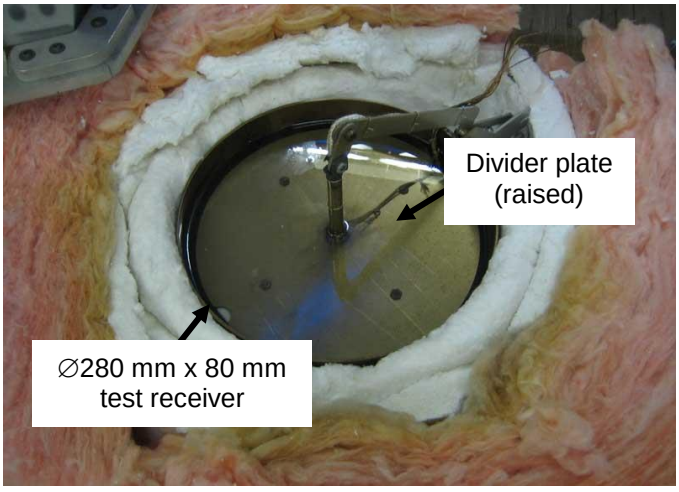

Fig. 3: Divider plate test receiver: nitrate solar salt

Figure 4 depicts the temperature distribution of the aforementioned test receiver for different positions of the divider plate. The initial temperature at $t = 0$ (not shown) was nearly isothermal; various radial thermocouple locations indicated the temperature distribution was essentially one-dimensional along the receiver's axis during optical heating. The divider plate succeeds in providing excellent thermal separation between the optically heated upper (hot) and bottom (cold) sections. The bare stainless steel top surface of the divider plate absorbs much more energy than the visibly transparent salt; as a result the hottest region of the receiver is the top surface of divider plate. This temperature inversion is excellent for establishing natural convection cells in the top region and promoting uniform, isothermal conditions which maximize thermal storage in a given volume of salt.

Ongoing experiments are examining the transient behavior of a moving divider plate with salt flow from hot to cold, simulating real world operating conditions with heat extraction. However, in this small scale test system the light mostly penetrates to the divider plate – and cannot provide insight to how a full scale machine would truly work. As a result, numerical modeling is required to design the full scale tank and divider plate system, and then testing of a deep tank system.

CONCLUSIONS

A CSP system has been presented where hillside mounted heliostats direct sunlight into a volumetric absorption molten salt receiver with integral storage. The CSPonD DAR simplifies the system by eliminating the conventional tower based receiver, materials driven temperature limits on receiver structure, remote thermal storage system and high pressure pumps. Volumetric absorption into the passive molten salt pond results in increased performance and durability, enabling higher working fluid temperatures and improved power cycle efficiency.

The receiver pond is internally insulated with firebrick and has a relatively small aperture and a refractory lined lid, whereby salt vapor condenses on the inner surface to form a self-healing reflective surface. This construction reduces secondary heat losses and avoids thermal fatigue associated with boiler tube-type receivers while achieving high temperatures needed for efficient power generation. In addition, the receiver volume also acts as the thermal storage volume. Hot salt is pumped from the top of the tank through a heat exchanger and then back into the bottom of the tank. An insulated plate provides an additional thermal barrier between the thermally stratified hot and cold layers within the tank, and the barrier is moved axially up and down to provide high temperature thermal energy even as the average temperature of the salt in the tank decreases when the sun is not shining.

Lab-scale molten salt DAR experiments indicate viability of the concept; the next step is to design a 20-100 kW_t test receiver that has an aperture size to receive light from a research heliostat field. This receiver would, however, be designed with the full anticipated depth of a larger system, so the optical penetration and convective mixing properties anticipated for the MW_e sized CSPonD system can be evaluated.

CSPonD systems are expected to benefit from reduced capital costs and result in lower levelized costs for energy produced. A majority of the cost in CSP systems is the heliostat field, and although hillside beam-down geometry results in additional cosine losses compared to conventional beam-up configurations, the CSPonD receiver is expected to exhibit increased collection efficiency and availability. More significantly, the capital cost for a CSPonD receiver is reduced with extensive use of low-cost refractory materials, low-cost salts and by eliminating the parasitic energy draw of high pressure, high temperature power tower heat transfer fluid pumps.

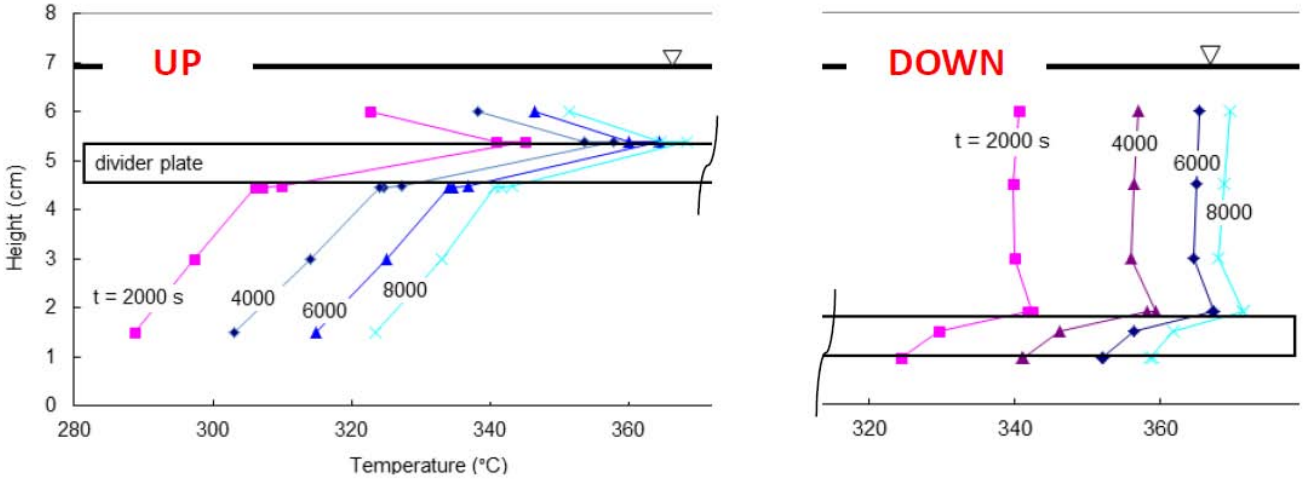

Fig. 4: Temperature distribution of nitrate solar salt heated optically; divider plate up (L) and down (R)

ACKNOWLEDGMENTS

This work is part of an interdisciplinary collaboration between the Cyprus Institute, the University of Illinois at Urbana Champaign, the Electricity Authority of Cyprus, and the Massachusetts Institute of Technology. Generous graduate student fellowships were provided by the Chesonis Family Foundation and the Bill and Melinda Gates Foundation. The authors would also like to thank Prof. Jeffrey M. Gordon of Ben-Gurion University of the Negev and Dr. Steve Fantone of Optikos, Inc. for their optical engineering insights, and Prof. Alan Hatton of MIT for his evaluation of the viability of a nanoparticle-based approach to light absorption in molten salts.

REFERENCES

[1] Stoke W., 1999, Solar Two Central Receiver, P600-00-017, California Energy Commission.

[2] Reilly H. E., and Kolb G. J., 2001, An Evaluation of Molten-Salt Power Towers Including Results of the Solar Two Project, Sandia National Labs, Albuquerque, NM; Livermore, CA, SAND2001-3674.

[3] Viebahn P., Kronshage S., and Lechon Y., 2008, Deliverable n 12.2-RS Ia" Final report on technical data, costs, and life cycle inventories of solar thermal power plants, NEEDS New Energy Externalities Developments for Sustainability.

[4] Diver R. B., 1987, "Receiver/Reactor Concepts for Thermochemical Transport of Solar Energy," J. Sol. Energy Eng., **109**(3), pp. 199-204.

[5] Bohn M. S., and Green H. J., 1989, "Heat transfer in molten salt direct absorption receivers," Solar Energy, **42**(1), pp. 57-66.

[6] Smith D. C., Rush E. E., Matthews C. W., Chavez J. M., and Bator P. A., 1992, Report on the test of the molten-salt pump and valve loops, SAND91-1747.

[7] Rabl A., 1976, "Tower reflector for solar power plant," Solar Energy, **18**(3), pp. 269-271.

[8] Epstein M., and Segal A., 1998, "A new concept for a molten-salt receiver/storage system," Proceedings of Solar 98: Renewable Energy for the Americas, 14-17 June 1998, ASME, New York, NY, USA, pp. 383-90.

[9] Segal A., and Epstein M., 2003, "Solar ground reformer," Solar Energy, **75**(6), pp. 479-490.

[10] Yogev A., 1997, "Heat storage device," US Patent 5685289.

[11] Epstein M., Segal A., and Yogev A., 1999, "A molten salt system with a ground base-integrated solar receiver storage tank," Le Journal de Physique IV, **9**(PR3).

[12] Yogev A., Kribus A., Epstein M., and Kogan A., 1998, "Solar tower reflector systems: a new approach for high-temperature solar plants," International journal of hydrogen energy, **23**(4), p. 239–245.

[13] Medrano M., Gil A., Martorell I., Potau X., and Cabeza L. F., 2010, "State of the art on high-temperature thermal energy storage for power generation. Part 2–Case studies," Renewable and Sustainable Energy Reviews, **14**(1), p. 56–72.

[14] Kelly M. J., Hlava P. F., and Brosseau D. A., 2004, Testing thermocline filler materials and molten-salt heat transfer fluids for thermal energy storage systems used in parabolic trough solar power plants.

[15] Herrmann U., Kelly B., and Price H., 2004, "Two-tank molten salt storage for parabolic trough solar power plants," Energy, **29**(5-6), p. 883–893.

[16] Gabbrielli R., and Zamparelli C., 2009, "Optimal Design of a Molten Salt Thermal Storage Tank for Parabolic Trough Solar Power Plants," J. Sol. Energy Eng., **131**(4), p. 041001.

[17] Slocum A. H., Buongiorno J., Forsberg C. W., Codd D. S., and Paxson A. T., 2010, "Concentrated Solar Power System", PCT Patent Application PCT/US10/49474.

[18] Slocum A. H., Codd D. S., Buongiorno J., Forsberg C. W., McKrell T., Nave J. C., Papanicolas C., Ghobeity A., Noone C., Passerini S., Rojas F., and Mitsos A., 2011, "Concentrated Solar Power on Demand," Solar Energy, *in press*.

[19] Noone C. J., Ghobeity A., Slocum A. H., Tzamtzis G., and Mitsos A., 2011, "Site selection for hillside central receiver solar thermal plants," Solar Energy, **85**(5), pp. 839-848.

[20] Passerini S., 2010, "Optical and Chemical Properties of Molten Salt Mixtures for Use in High Temperature Power Systems," SM thesis, Massachusetts Institute of Technology.

[21] Ghobeity A., and Mitsos A., 2009, "Optimal Use of Solar Thermal Energy for Combined Power Generation and Water Desalination," Proceedings of Distributed Renewable Energy Sources in the Mediterranean Region (DISTRES 2009), Nicosia, CY.

[22] Mehrkam Q. D., 1967, "An Introduction to Salt Bath Heat Treating," Tooling & Production, **June/July 1967**(June/July).

[23] Allman W. A., Smith D. C., and Kakarala C. R., 1988, "The design and testing of a molten salt steam generator for solar application," Transactions of the ASME. Journal of Solar Energy Engineering, **110**(1), pp. 38-44.

[24] Forsberg C. W., and Moses D. L., 2009, Safeguards Challenges for Pebble-Bed Reactors (PBRs): Peoples Republic of China (PRC), Oak Ridge National Laboratory (ORNL).

[25] Copeland R. J., and Green J., 1983, "Raft thermocline thermal storage," Proceedings of the 18th Intersociety Energy Conversion Engineering Conference, 21-26 Aug. 1983, AIChE, New York, NY, USA, pp. 1801-5.

[26] Copeland R. J., West R. E., and Kreith F., 1984, "Thermal energy storage at 900C," 19th Intersociety Energy Conversion Engineering Conference (Cat. No. 84CH2101-4), 19-24 Aug. 1984, American Nucl. Soc, LaGrange Park, IL, USA, pp. 1171-5.

[27] Codd D. S., Carlson A., Rees J., and Slocum A. H., 2010, "A low cost high flux solar simulator," Solar Energy, **84**(12), pp. 2202-2212.
[28] Siegel R., 2002, Thermal Radiation Heat Transfer, Taylor & Francis, New York.
[29] Duffie J. A., 2006, Solar Engineering of Thermal Processes, Wiley, Hoboken, N.J.
[30] Bradshaw R. W., Dawson D. B., De La Rosa W., Gilbert R., Goods S. H., Hale M. J., Jacobs P., Jones S. A., Kolb G. J., Pacheco J. E., Prairie M. R., Reilly H. E., Showalter S. K., And Vant-Hull L. L., 2002, Final Test and Evaluation Results from the Solar Two Project, Sandia National Labs, Albuquerque, NM; Livermore, CA, SAND2002-0120.

ANNEX A

CSPOND RECEIVER CAPTURE EFFICIENCY

NOMENCLATURE

A	surface area
D	diameter
F_{1-2}	view factor from surface 1 to surface 2
h	convection coefficient
ΔH_{vap}	enthalpy of vaporization of salt
n	index of refraction
R	reflection coefficient
T	temperature
T_∞	ambient temperature
Q	heat flow rate
Q_{in}	gross solar input
γ	rate of salt vaporization per unit area
ε	emissivity
$\eta_{capture}$	capture efficiency
θ_i	incident angle
θ_t	transmitted angle
θ_r	reflected angle
ξ	tank storage efficiency
σ	Stefan-Boltzmann constant
ϕ	beam-down angle
Φ	input flux concentration

Subscripts

a	aperture
conv	convective
ip	illuminated pond
l	lid
p	nominal/design pond, *p*-polarized
rad	radiative
s	*s*-polarized
salt	salt
tank	tank
vap	vaporization

RECEIVER EFFIENCY CALCULATION

A simplified model can be used to give first order efficiency estimates for the proposed CSPonD receiver. Key assumptions include:

- Uniform, collimated input flux is completely captured by the aperture
- Lid is well insulated to the outside environment
- Energy directed to the lid is completely absorbed
- Air/salt vapor above the pond is at the lid temperature
- No mass transfer through aperture (i.e., salt vapors from pond surface condense onto lid)

"Capture Efficiency" is defined as the fraction of incoming energy retained by the receiver – used to heat both the pond and the lid. Unique to CSPonD systems are these dual zones for heat rejection available at different temperatures. Operators can choose to utilize low temperature lid designs for power cycle preheating, or hybrid needs such as RO or MED desalination feedwater heating. CSPonD receivers with high temperature lid heat may even be employed for primary power cycle heating, followed by superheating with the higher temperature molten salt heat reservoir.

Fig. A1 shows the design inputs used to calculate CSPonD receiver collection efficiency. The collected energy can be separated into net amounts which are absorbed into salt and into the lid.

The minimum aperture area is determined by system sizing and input flux concentration, Φ

$$A_a = Q_{in} / \Phi \tag{2}$$

and is used to calculate the system's geometrical view factors needed for accurate radiative loss estimates to the environment. For a central heliostat located on the optical axis of the receiver aperture, the input flux will be restricted to an ellipse of major axis, D_{ip}, projected on the salt surface

$$D_{ip} = D_a / \sin \phi \tag{3}$$

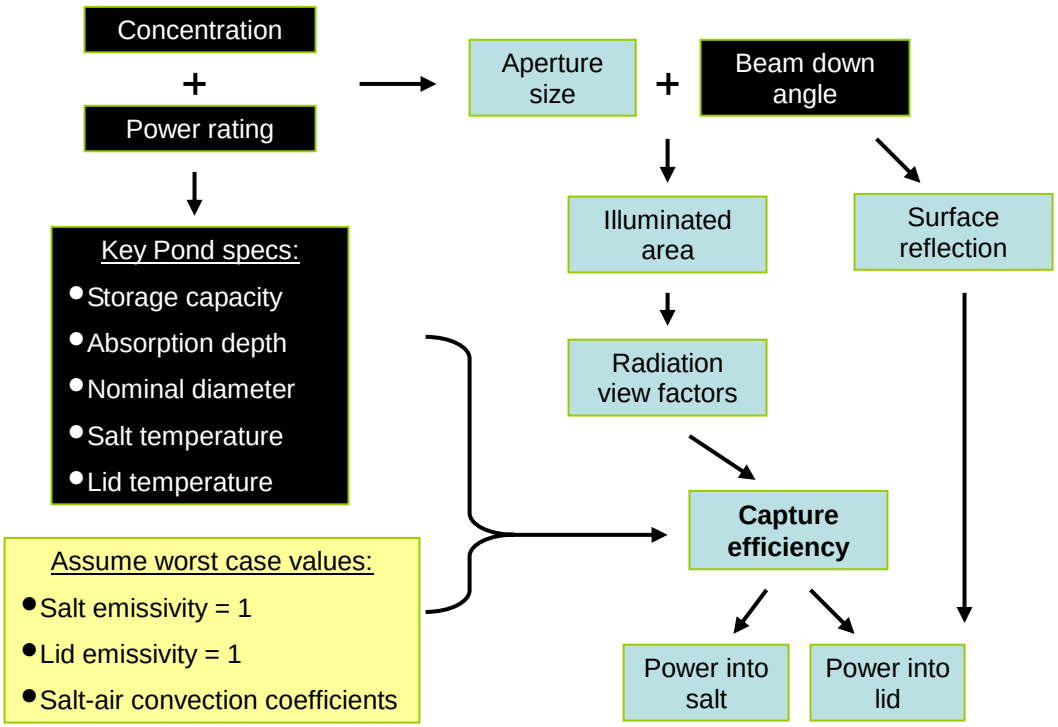

Fig. A1: Schematic of calculation of CSPonD receiver "capture efficiency"
System design parameters are indicated in black boxes

where ϕ is the nominal beam-down angle measured from horizontal (Fig. A2).

Clearly, if D_{ip} is greater than or equal to the nominal design pond diameter, D_p, a portion of the incoming light will 'spill' onto the inside of the lid structure. A hemispherical lid cover is assumed, which has a surface area

$$A_l = 2\,\pi\,D_l^2 \tag{4}$$

where

$$D_l = \min(\,D_{ip}\,,\,D_p\,) \tag{5}$$

and

$$A_p = \pi/4 \cdot D_l^2 \tag{6}$$

The following view factor relationships can be derived using the radiation view factor for any finite area of any shape on interior of hemisphere to the hemisphere's entire base [28], the view factor reciprocity relationship, and the fact that the pond surface "sees" only the lid and aperture areas

$$F_{p\text{-}l} = 1 - \tfrac{1}{2}\,(A_a/A_p) \tag{7}$$

$$F_{p\text{-}a} = \tfrac{1}{2}\,(A_a/A_p) \tag{8}$$

$$F_{l\text{-}a} = \tfrac{1}{2}\,(A_a/A_l) \tag{9}$$

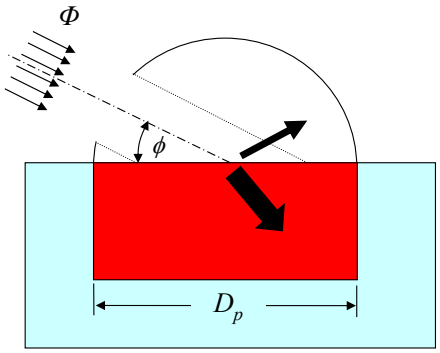

Fig. A2: Simplified CSPonD DAR geometry

The radiative heat transfer from the pond to the lid, from the pond to the aperture, and from the lid to the aperture can be found using

$$Q_{rad,1\text{-}2} = F_{1\text{-}2}\, A_1\, \varepsilon_1\, \sigma (\, T_1^{\,4} - T_2^{\,4}\,) \tag{10}$$

Emissivities of unity were assumed to set an upper bound on heat losses through the aperture; in physical systems the salt surface is expected to have an emissivity ~ 0.9, and the lid may have emissivity values ranging from 0.1-0.9. In fact, the lid emissivity, temperature and geometry may be tailored throughout the lid's surface to lower the overall heat losses to the environment.

The convective heat transfer from the pond to lid and from the lid to the aperture can be approximated as

$$Q_{conv,1\text{-}2} = h\, A_1\, (\, T_1 - T_2\,) \tag{11}$$

where standard correlations for a heated surfaces can be used to find estimates for the natural convective coefficient, *h*, for the salt and lid geometry.

An evaporation rate, γ, defined as the mass of salt per exposed surface area per unit time vaporized, can be assumed to calculate vaporization heat transfer from the pond's surface

$$Q_{vap} = \gamma\, \Delta H_{vap}\, A_p \tag{12}$$

Conductive heat loss through the tank walls can be assumed as a percentage of the overall system capacity

$$Q_{tank} = \xi\, Q_{in} \tag{13}$$

A portion of the incoming concentrated light is reflected off the molten salt-air interface. This reflected fraction can be calculated from the Fresnel equations describing light as it moves between media of different refractive indices. The reflection coefficients for *s*- and *p*- polarized light are

$$R_s = \left[\frac{\sin(\theta_t - \theta_i)}{\sin(\theta_t + \theta_i)} \right]^2 \tag{14}$$

$$R_p = \left[\frac{\tan(\theta_t - \theta_i)}{\tan(\theta_t + \theta_i)} \right]^2 \tag{15}$$

The angles that the incident, reflected and refracted rays make to the normal of the interface are given as θ_i, θ_r and θ_t, respectively, and related by Snell's Law and the law of reflection:

$$n_{salt} \sin\theta_t = n_{air} \sin\theta_i \tag{16}$$

$$\theta_r = \theta_i \tag{17}$$

where

$$\theta_i = 90° - \phi \tag{18}$$

Since the incident light is unpolarized, containing an equal mix of *s*- and *p*-polarizations, the reflection coefficient, *R*, is

$$R = \left(R_s + R_p\right)/2 \tag{19}$$

The incoming power absorbed directly into the salt becomes

if $D_{ip} \le D_p$:

$$Q_{direct,salt} = Q_{in}\,(1 - R) \tag{20}$$

if $D_{ip} > D_p$:

$$Q_{direct,salt} = Q_{in}\,(1 - R) \cdot (D_p / D_{ip})^2 \tag{21}$$

The incident power reflected and spilled onto the lid is

$$Q_{reflect} = Q_{in} - Q_{direct,salt} \tag{22}$$

The net power to the salt is

$$Q_{salt} = Q_{direct,salt} - (Q_{rad,p\text{-}a} + Q_{tank}) - (Q_{vap} + Q_{conv,p\text{-}l} + Q_{rad,p\text{-}l}) \tag{23}$$

and similarly, the net power to the lid becomes

$$Q_{lid} = Q_{reflect} - (Q_{rad,l\text{-}a} + Q_{conv,l\text{-}a}) + (Q_{vap} + Q_{conv,p\text{-}l} + Q_{rad,p\text{-}l}) \tag{27}$$

The capture efficiency, $\eta_{capture}$, can be calculated as

$$\eta_{capture} = \frac{Q_{in} - Q_{losses}}{Q_{in}} \tag{28}$$

where

$$Q_{losses} = Q_{rad,l\text{-}a} + Q_{conv,l\text{-}a} + Q_{rad,p\text{-}a} + Q_{tank} \tag{29}$$

Using nominal design values for a 2500 m^3 (600 $MW_t h$) storage system, 65 MW_t power rating and a 21.4° average beam down angle, overall CSPonD capture efficiencies can be found (Fig. A3). The high (chloride) and low (nitrate) temperature designs for different salts are presented, each with an assumed lid temperature set at the freeze point of its respective salt. At this lid temperature, a self-sustaining salt vapor condensation and recycling loop is expected to develop within the receiver's

cavity, limiting heat and mass transfer outside of the receiver. For comparison, measured Solar I and Solar II peak and average receiver collection efficiencies are shown [1,29,30].

Conventional tube based-receivers, such as those used in Solar I and II, are designed so that incoming flux strikes the tube near-normally to its surface. Unfortunately, a fraction of the incident light is reflected off the receiver's surface and cannot be recaptured. Much effort and costs are spent applying solar absorption coatings, or relying on surface oxides to grow and reduce the tube's reflectivity – but the absorptivity of the tube surface presents an upper bound to tube-based receiver efficiency. In contrast, the proposed CSPonD receiver captures reflected light with the lid, converting it to useful heat, or depending on lid temperature and construction, redirecting it back into the salt. Both designs are subject to radiative and convective losses – but with the proposed CSPonD receiver's smaller aperture, overall efficiency is superior in high concentration systems.

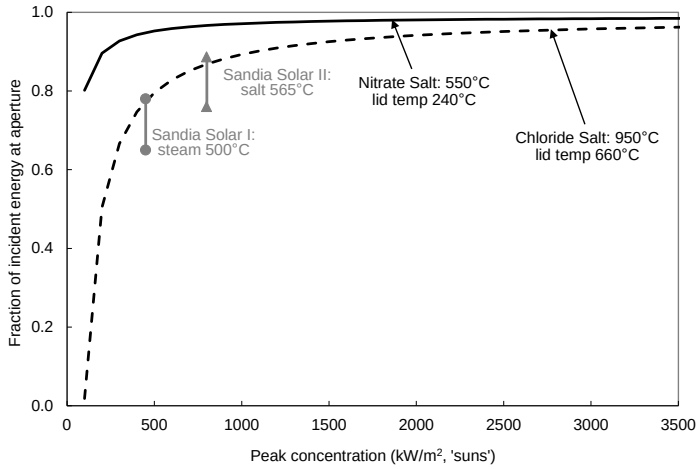

Fig. A3: CSPonD DAR capture efficiency
Nitrate salt: pond at 550°C, lid at 240°C
Chloride salt: pond at 950°C, lid at 660°C

Figures A4-A6 examine the sensitivity of the 50 MW_e nitrate salt (550°C) CSPonD receiver's efficiency to various design parameters: nominal pond diameter, average beam down angle, and lid temperature. Varying the nominal pond diameter can drastically shift the amount of energy directed to the pond or lid (Fig. A4). Three receiver regimes are illustrated: (a) Pond undersized: a portion of the incoming is light spilled onto lid walls, the amount of this spillage and heat gain onto the lid decreases as the input flux concentration increases; (b) Pond exactly sized for a specific aperture and particular beam-down geometry; (c) Pond oversized: the exposed pond surface can be reduced to match the illuminated area, increasing concentration enables further reductions in exposed salt surface area, further reducing losses and heat gain onto the lid. It is interesting to note at low input flux concentrations, nearly all of the captured energy is available at the lid; very little is directed to the molten salt pond. Low concentrations require large apertures and large illuminated pond areas, both of which increase losses from the molten salt to the lid and the environment.

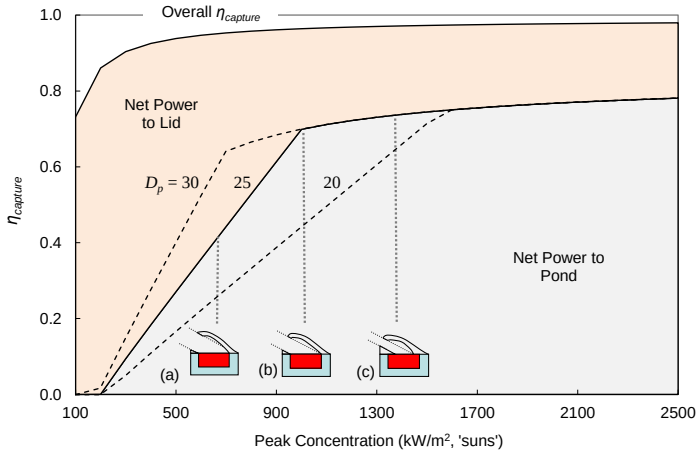

Fig. A4: Effect of pond diameter on capture efficiency

Similarly, Fig. A5 shows larger beam down angles (i.e. steeper hillsides for the heliostat field) are effective at directing more of the incoming energy into the salt. A steeper beam down angle has two effects: firstly, the illuminated or projected area of the aperture on the horizontal molten salt pool is decreased, reducing required exposed salt area and subsequent losses. Secondly, Fresnel reflections off of the salt surface are reduced, reducing the fraction of incident light which is reflected onto the lid. The net heat to the lid approaches Fresnel reflection limits for unpolarized light at very high concentrations.

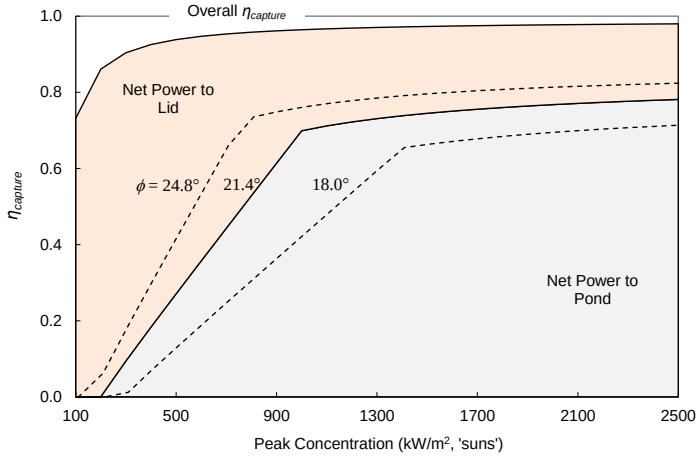

Fig. A5: Effect of beam down angle on capture efficiency

Fig. A6 shows reduced capture efficiency with increasing lid operating temperatures. This is primarily due to larger radiative and convective losses from the hotter lid out of the aperture. However, a higher lid temperature reduces the radiative heat transfer from the salt pond to the lid – effectively keeping more heat in the salt.

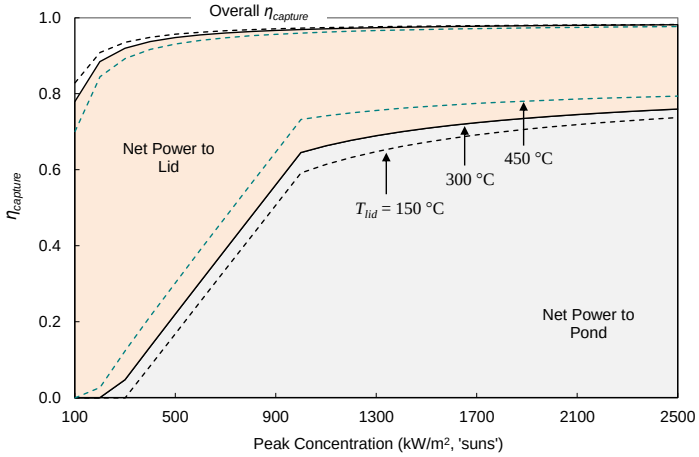

Fig. A6: Effect of lid internal temperature on capture efficiency